The role of spectral multimodality in wave climate design

Layla Loffredo * and Jaak Monbaliu

Hydraulics Laboratory, Katholieke Universiteit Leuven, Belgium

Elzbieta Bitner-Gregersen

Department for Strategic Research, Det Norske Veritas, Veritasveien 1, Høvik 1322, Norway

Alessandro Toffoli

Swinburne University of Technology, PO Box 218, Hawthorn, Victoria 3122, Australia

1. Introduction

In design practice there is the need for summarizing the spectral information into parameters, which are integrated over the spectrum. However this synthesis does not include knowledge about the different meteorological components that have generated the sea state. Spectral multimodality describes the co-existence, within the sea state, of locally generated wind sea and swell systems, which are associated to independent meteorological events. Such conditions are referred to mixed seas. For certain marine operations and design practices, there is a need for statistical information about the combination of different wave systems. Design practice has shown that reliable directional data allow cost optimization in offshore facilities (Jonathan et al., 2008) by reducing the inconsistencies in design criteria due to omni-directional approaches. Multimodal sea states can have a significant impact on design and operability of fixed and floating offshore platform (Ewans et al., 2006). Beside offshore applications, coastal hazard assessment can benefit as well from the multi-modal nature of wave spectra. As illustrated by Bradbury et al.(2007) for a location along the English Channel during storm events, beach response is better described by the spectral characteristics rather than by the integrated parameters.

The directional wave energy spectrum $S(f, \theta)$, describes the distribution of the energy variance over frequencies f and directions θ. There are several methods to separate a spectrum into wave systems. Spectral partitioning permits identifying the wind sea contribution and distinguish between swell systems derived from different storms. The concept was initially proposed by Gerling (1992), Hasselmann et al. (1996) modified the scheme and proposed an approach to allow comparison between SAR and WAM wave model spectra. The partitioning schemes that came after often refer to Hasselmann's idea of looking at the wave spectra as inverted catchment area. Following the hydrological analogy the local maxima of the wave spectrum are identified by steepest ascent path and regarded as morphological features. Voorrips et al. (1997) extended this application to the assimilation of pitch-and-roll buoys and more recently Hanson and Phillips (2001) and Aarnees and Krogstad (2001) employed Hasselmann's scheme and proposed techniques to track and identify swell sources.

In this paper Hasselmann's scheme is adopted and applied to a study area located in the Norwegian Sea. In complex sea states the assignment to single wave systems, gives way to different wave climates. Some criteria to facilitate the interpretation of the obtained climate are presented.

2. The partitioning scheme

a. *Overview of the method*

The spectral partitioning procedure has been implemented into the Multiple Seas (MuSeas) toolbox (Loffredo, 2009), developed in a MATLAB environment. The scheme is defined by 3 main steps: partitioning the spectra into wave systems, combining systems (optional) and assigning wind sea and swell to the identified systems according to a wave age criterium. For the latter step wind information is required. Although the sequence of the steps does not change, there are a number of alternatives that the user can select to organize the resulting output. The inverse watershed concept applied to a directional wave spectrum, suggests that local energy maxima can be identified by following the steepest ascent path from every grid point. All the neighboring points with lower energy conforming this condition, are clustered into a subset. Each subset, which constitutes a partition, is associated with a portion of energy from the total spectrum (corresponding to the subcatchment area) with a peak direction and a peak frequency. The watershed algorithm proposed in Portilla et al.(2009) has been implemented for the present study.

* *Corresponding author address:* Layla Loffredo
Hydraulics Laboratory, Katholieke Universiteit Leuven
Kasteelpark Arenberg 40, Heverlee 3001, Belgium
E-mail: layla.loffredo@bwk.kuleuven.be

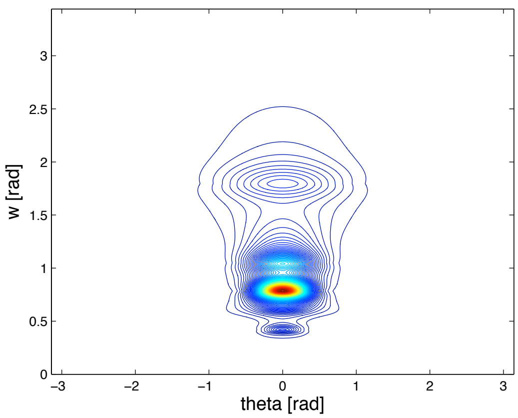

(a) Systems with same direction of provenance

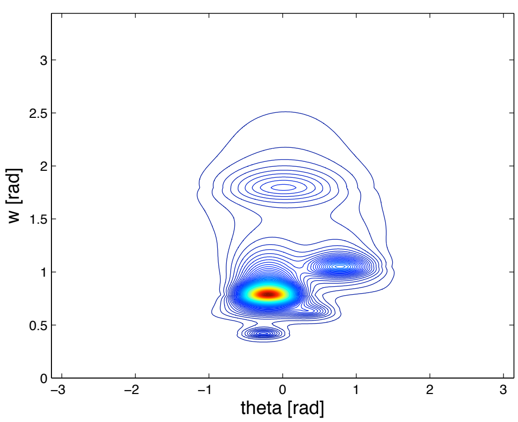

(b) Systems with different direction of provenance

Fig. 1. 2D directional spectra with more than 2 wave systems

b. Identifying the wave systems

Events that might affect the performance of the algorithm executing the spectral partitioning have been analysed. Possible complications that the algorithm might encounter are related to wave systems coming from the same direction as illustrated in figure 1(a) and to the presence of more than two swell systems. In the latter case what is critical is the amount of energy contained in tertiary and quaternary swells. However if the wave systems have approximately the same amount of energy the algorithm can still identify with accuracy all the peaks, even in the case of systems close in direction (figure 1(b)). Another limitation has been observed in the case of bimodal seas with a wind sea and a swell system close in peak frequency. The algorithm cannot identify both peaks one is hidden under the dominant system, even though it contains a relevant amount of energy. One could call this a condition of hidden seas. The morphological feature, as illustrated in figure 2 is not clearly visible. Despite these limitations, the algorithm is a robust core for the partitioning scheme.

c. Combining the systems

As emerges from literature, there is not a single procedure for combining wave systems (Hasselmann et al., 1996; Voorrips et al. 1997; Hanson and Phillips, 2001). The choice of the criteria is at one's discretion. However it has as basis an interpretation of morphological attributes present in the spectrum, such as the distance between two peaks, the position of the saddle point or an energy threshold. As remarked by Aarnes and Krogstad (2001) the selection of the control parameters is crucial but at the same time it is difficult to evaluate how physically correct they are. The magnitude of the energy threshold has a direct effect on the number of wave systems involved and setting a lower threshold might include in the output also noise and spurious peaks. Herewith the procedure allows merging if the energy content is less than 5% of the total energy and if two adjacent peaks are located at one (or two) grid points away from each other. If the above conditions apply, then the two partitions are merged and so their energy content. The resulting wave systems can be organized according to different principles, depending on the purpose of the analysis. Sorting the partitions according to descending energy contents may be enough for certain marine applications. Once defined a maximum number of wave systems, the superfluous partitions are eliminated. This operation can be seen as a tradeoff. On one side it is a simplification, but on the other hand it limits the erroneous merging of systems that are not physically related. A energy cut off is always computed during this passage to monitor any relevant energy loss. From the experience in the current study the reduction has never been higher than 0.3-0.4% the energy.

d. Assigning

A further step is the assignment for each partition to wind sea or swell. According to a wave age criterium the wind sea region fulfills the following relation:

$$\alpha(U/c)cos(\theta - \varphi) > 1 \tag{1}$$

where α is a calibration factor, U the wind speed, $c = c(f)$ the phase speed, θ the wave direction and φ wind direction. Equation (1) has been adopted with different adjustements by several authors. For this reason three formulations have been selected to illustrate the dissimilarity in assigning wind sea and swell. Hasselmann et al. (1996) proposed a factor α equal to 1.3 and takes into account peak frequencies and direction. On the other hand Bidlot (2001) and Hanson and Phillips (2001) utilized mean parameters. Bidlot (2001) suggested a factor α of 1.2, while Hanson and Phillips (2001) allow a larger region of the 2D spectrum to be under the influence of the wind by increas-

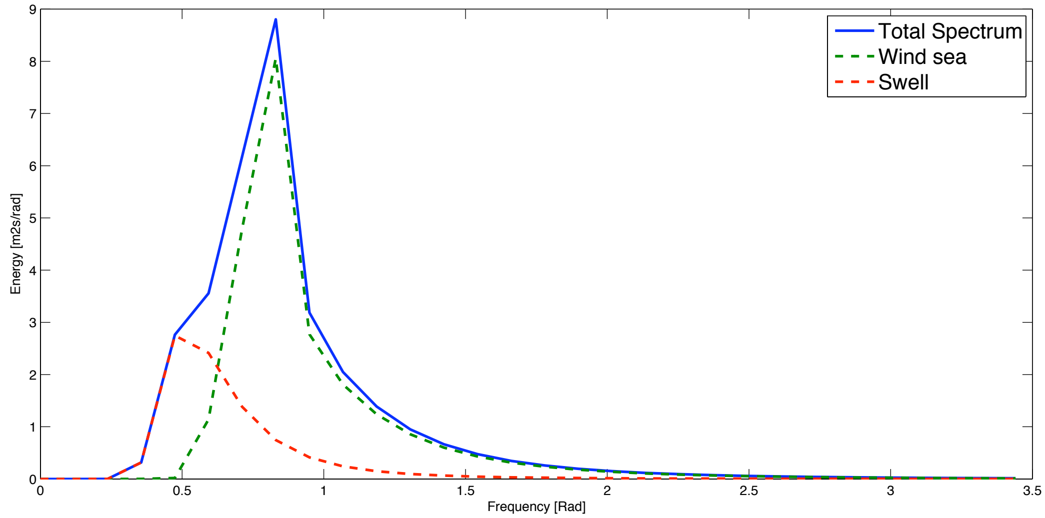

Fig. 2. Hidden seas

ing the factor up to 1.5. Typically a wind sea and two swell systems (primary and secondary, possibly tertiary if no wind sea is detected) are designed as main sea states features.

3. Analysis of Tromsøflaket wave climate

a. Data description

A homogeneous 20 years reanalysis dataset has been employed to describe the wave climate. WAM model simulated wave spectra and integrated parameters have been retrieved from the dataset ERA-Interim, one of the newest products of the European Centre for Medium-Range Weather Forecasts (ECMWF). As shown in Simmons et al. (2006) the main advances of the ERA-Interim over the ERA-40 embrace increased horizontal resolution (1°x1°), improved model physics, data quality control on the experience from ERA-40 and changes in the use of observations, such as a new and more uniform ERS altimeter wave height dataset. The time span analysed goes from 1989 till 2008, with a time resolution of 6h. The wave spectral resolution consists of 24 direction and 30 frequency bins. The direction array has regular resolution (15°) and the frequency band is expressed in logarithmic scale ($\triangle f/f = 0.1$), meaning that the frequency interval, which goes from 0.0345 till 0.5476 Hz, is not constant. For more details about the wave model configuration see Bidlot (2001).
The location Tromsøflaket (lat 71° lon 18.75°) selected for illustration is situated offshore in the Norwegian sea.

b. Separation based on energy content

The wind rose plot illustrated in figure 3(a) provides information about wind speed and directions. This type of plots are very functional to condense large amount of data and to yield a very clear overview on the dominant patterns. The length of each slice is proportional to the frequency of occurence, in addition a color scale indicates the wind speed class of intensity. The same type of plot has been adopted also for other variables, such as significant wave height ($Hm0$) and peak period (Tp). A classical way to examine wave climate is presented in figure 3(b) as reference. In this situation the wave spectra are treated as unimodal, meaning that a single peaked spectrum is assumed. Significant wave height distribution appears to be consistent with the wind pattern (figure 3(a)) and the coast alignment. Dominant directions are observed in the SW sector. Wave heights larger than 6m are expected from most directions. After processing the data with the MuSeas scheme, the resulting wave systems are organized according to the descending energy criterion and a thresholding is applied twice. First systems that are detected to be with a energy content less than 5% and close (by one or two grid points) in direction and frequency are joined with the dominant system. Second a maximum number n of wave systems is requested by the user, thus all the systems $n+k$ are eliminated. The number k in some circumstances can be up to 5 or 6, but it is never associated with relevant amount of energy. To monitor the energy neglected a quota is computed every time. In the present work the maximum number of systems allowed has been settled to 3, eliminating 0.0145% of the total energy.
In figure 3(c) and figure 3(d) also the wave climate roses

for first and the second system are shown. The major element revealed is the different directional allocation for wave heights. The dominant direction 225° is more pronounced, for both the first and the second system. Figure 3(e) and 3(f)) show the peak period statistics. For the location Tromsøflaket most of the wave fields have a peak period larger than 10s.

c. Separation based on wind sea and swell assignment

An additional step is executed to the above described analysis by assigning wind sea and swell labels to each wave system detected. Different formulations for the wave age criterion exist, having in common the employment of wind fields. According to Hasselmann et al. (1996) wave trains are under the influence of wind sea if they fullfill the following relation:

$$1.3(U/c)cos(\theta - \varphi) > 1 \qquad (2)$$

where c is the phase speed at the peak frequency as derived from the linear theory of waves, U is the wind speed, θ the wave propagation direction and φ the wind direction. The formulation proposed by Bidlot (2001) is slightly different in the calibration factor and for considering mean parameters instead:

$$1.2(U/c)cos(\theta - \varphi) > 1 \qquad (3)$$

Note that Hanson and Phillips (2001) use a factor of 1.5 in equation 3 instead of 1.2 to allow a larger region to be forced by the wind defined as wind sea.

Results obtained with Hasselmann's formulation (1996) are displayed in figure 4. The wind sea rose plot in figure 4(a) exhibits a wide range of direction classes in full agreement with the wind distribution (figure 3(a)). Dominant directions are from NE and SW, where wave heights above 10m can be found. Wind sea occurs 32.6% of the times whereas the swell 90.7%, however in terms of energy quota the wind sea covers the 39.4% and swell 60.6%. The total swell 4(b) represents the sum of the primary and secondary swell components (figures 4(c) and 4(d)). In all three cases the predominant swell direction is very evident. The assessment of this feature can be beneficial for design especially in terms of optimization costs. Primary and secondary swell have same pattern distribution, but with a energy ratio of approximately 2.5. It is not to be excluded that in other locations the secondary swell distribution could assume different structure. As expected by applying different formulations for labeling wind sea and swell, different output are obtained. A 14 days period has been extracted for illustration. Figure 5 gives a simplified view of the sea states from 01-03-1995 to 14-03-1995; the first panel represents the wind vector, which can be regarded as reference. The following 3 panels illustrates the assignment results. Every wave age formulation (eq. 2 and 3) has its own grid. It is straightforward to individuate the dissimilarities: the use of mean parameters (eq. 3) allows to associate more systems to wind sea and in the case of a larger region of influence (Hanson and Phillips 2001) the number of wind seas increases. Overall, for the 20 years analysis, according to Hasselmann's relation 32.6% of the spectra are associated to wind sea, the portion increases to 35.7% with Bidlot and reaches 43.2% with Hanson and Phillips. A discrepancy of 10.6% could have a weight in the design process.

As mentioned in Quentin (2002) the main drawback of these formulations is related to fully developed wind seas with a small wind decay but still in the same direction of the wave field; if the new condition cannot satisfy the aforementioned relations, the old wind sea will be treated as swell and the new wind sea set to zero.

d. Comparison with ECMWF assignment

The 3 formulations described in section c have been compared with the wind sea and swell parameters provided by ECMWF. A major difference in the method is that ECMWF does the assignment for every grid point of the spectral domain, validating the relation (3) bin by bin. This procedure generates sistematically a wind sea component and a swell. Thus the first observation is that with the MuSeas scheme absence of wind sea or swell are allowed. The confront between the two procedures is displayed in figure 6, paying attention to the variation due to the formulations applied in c. Wind sea estimated with Hasselmann's formulation shows good agreement with ECMWF results. The two formulations that apply mean parameters (Bidlot, 2001 and Hanson and Phillips, 2001), exhibt less correlation with ECMWF results, in fact in some point a large discrepancy (up to 5m) is observed. Swell comparison shows larger bias (even 8m). This difference can be explained with the allocation into wind sea and swell done by default at ECMWF. Furthermore wind sea and swell events that are detected by ECMWF are not recognized at all by MuSeas. This means that 10m wind sea and 7m swell could be misinterpreted by the procedure here proposed. These circumstances have been investigated by extracting the spectra that fall under these conditions. A constraint is imposed for ECMWF wave heights larger than 2m. Results show that with Hasselmann's formulation 1725 wind sea spectra out of 29220 are misinterpreted, for Bidlot's and Hanson's, 2329 and 2131 respectively. For the swell 731 (Hasselmann), 1780 (Bidlot) and 2102 (Hanson) out of 29220.

e. Additional criteria for assignment

1) Wave steepness

Additional conditions can help the interpretation. Two spectral properties have been explored: wave steepness and

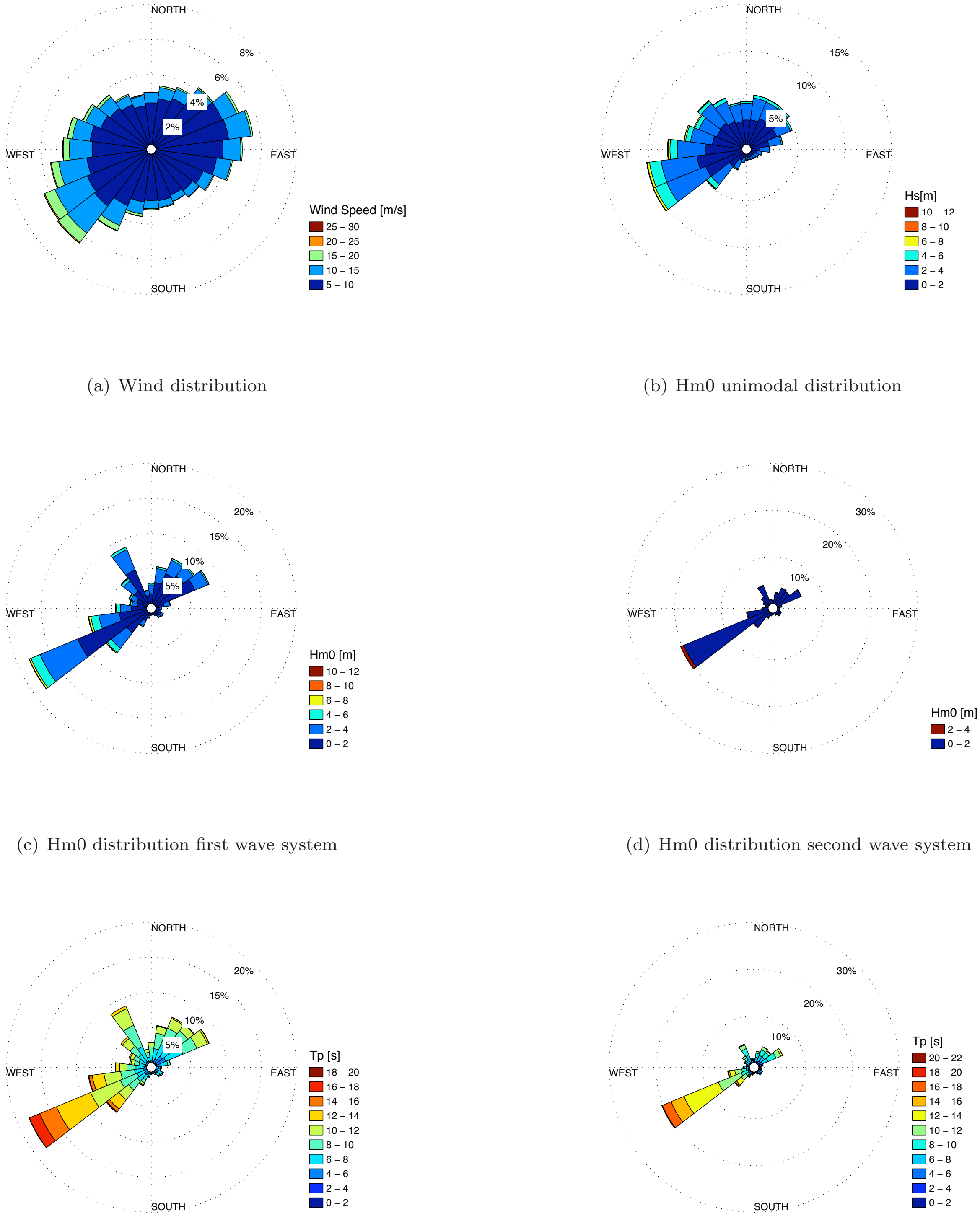

(a) Wind distribution

(b) Hm0 unimodal distribution

(c) Hm0 distribution first wave system

(d) Hm0 distribution second wave system

(e) Tp distribution first wave system

(f) Tp distribution second wave system

FIG. 3. Rose plot distributions based on 15° resolution. Directions indicate true North with the convention "coming from". Number of spectra analysed: 29220.

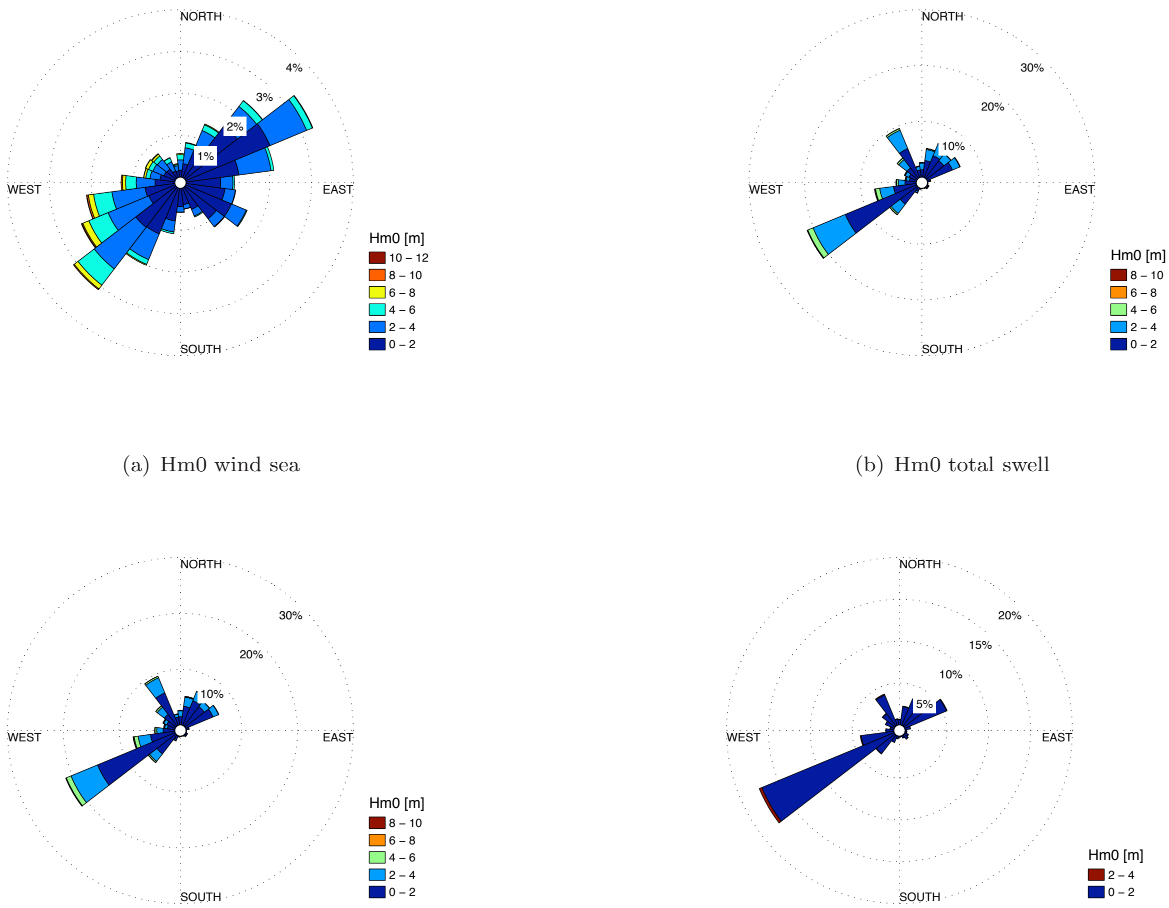

(a) Hm0 wind sea

(b) Hm0 total swell

(c) Hm0 primary swell

(d) Hm0 secondary swell

Fig. 4. Rose plot distributions for assignment according to Hasselmann's relation (1996) based on 15° resolution. Directions indicate true North with the convention "coming from". Number of spectra analysed: 29220.

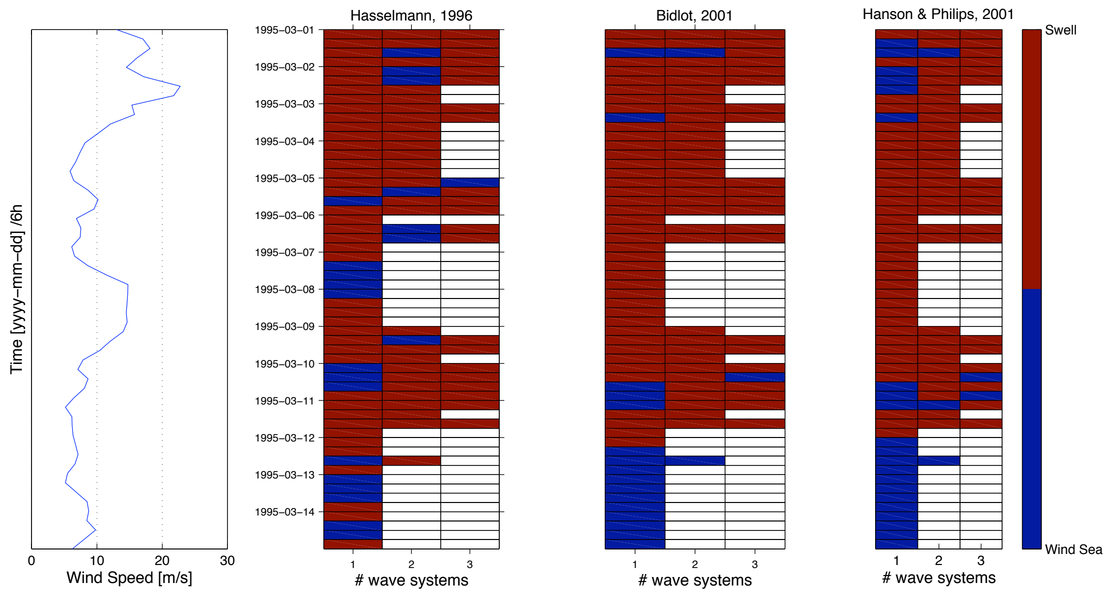

FIG. 5. Assignment to wind sea described with 3 formulations: Hasselmann et al. (1996), Bidlot (2001), Hanson and Phillips (2001). First plot represents wind vector. Each grid has 3 columns corresponding to the number of wave systems required, in blue assignment to wind sea, in red swell and no system detected in white.

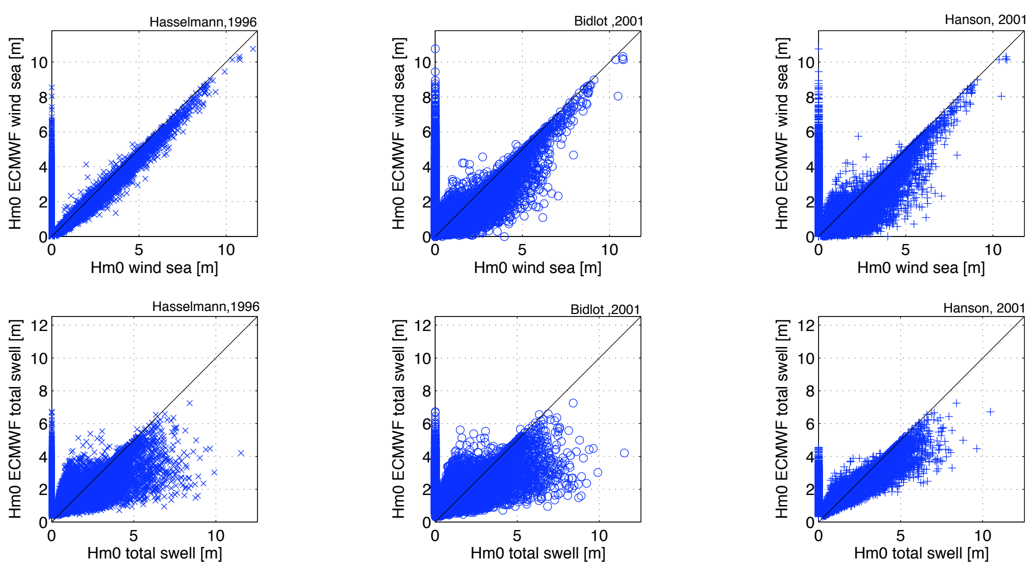

FIG. 6. Contrast for wind sea and swell estimations (MuSeas 3 formulations) and ECMWF data

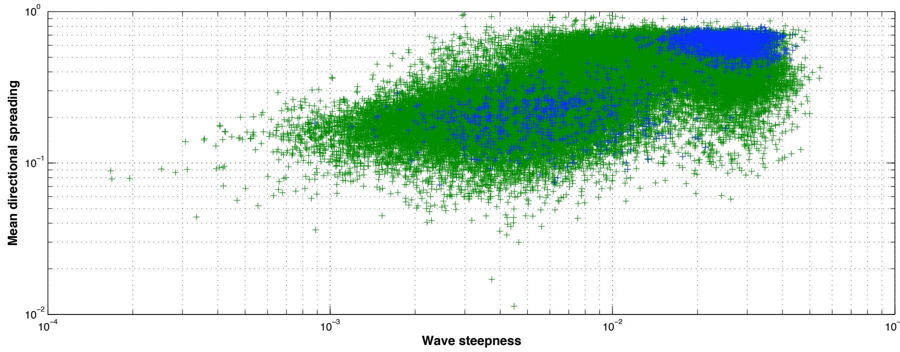

(a) In blue the extracted spectra for the wind sea interpretation

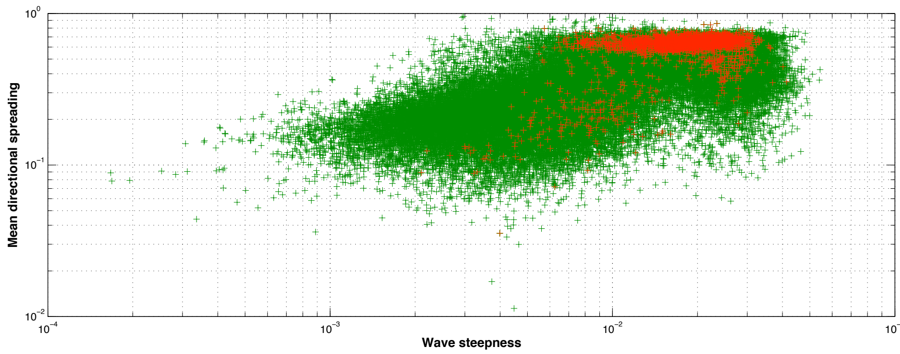

(b) In red the extracted spectra for the swell interpretation

FIG. 7. Correlation between wave steepness and directional spreading

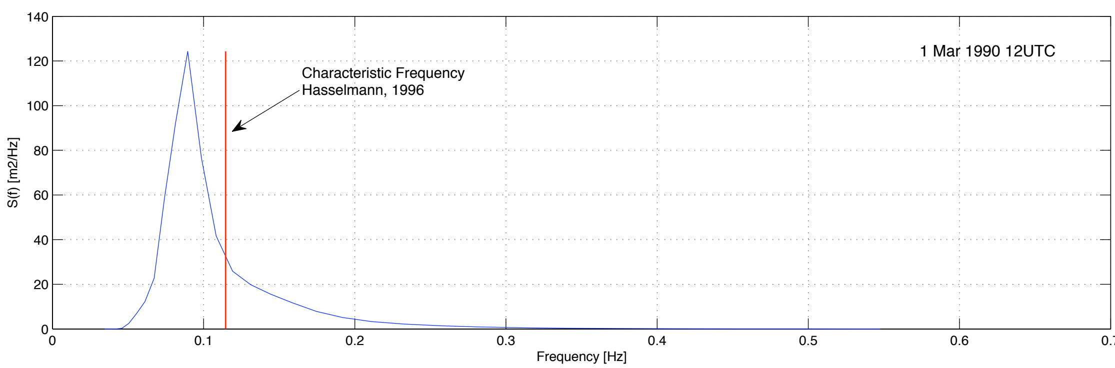

FIG. 8. Characteristic frequency for 1D spectrum

directional spreading. Besides a characteristic frequency is derived from the wave age criterion (eq. 1), this parameter assists into marking the passage from wind sea to swell. Wave steepness is defined according WMO (1998) as:

$$\xi = \frac{2\pi Hm0}{gT_{m_{-10}}^2} \tag{4}$$

where $Hm0$ is significant wave height and T_{m-10}^2 is energy wave period. As observed by Toffoli et al. (2005) wind dominated seas are characterized by higher steepness while swell dominated are less steep. Wind sea steepness reaches an asymptotic value due to the breaking limit.

2) Directional spreading

Here we investigate the directional spreading, which we define as follows:

$$\sigma = [2(1 - r_1)]^{1/2} \tag{5}$$

According to the relation presented by Bidlot (2001) the mean directional spread σ is the circular standard deviation of the directional spreading function. The parameter r_1 is used to compute the 1^{st} order Fourier coefficient of the spreading function and it is generally function of the frequency. In other words σ can describe how the wave energy is distributed over the directions. It assumes values between 0 and $\sqrt{2}$, whre 0 corresponds to a unidirectional spectrum and $\sqrt{2}$ for uniform spectrum.

Figures 7 show the relationship between wave steepness and mean directional spread. This pattern is consistent with the one proposed by Goda (2000), where a S_{max} spreading parameter is used instead. In green all the spectra are plotted, then in upper panel, those wind seas that were not recognized by the MuSeas procedure are superimposed. Similarly in the lower panel the extracted swell spectra are put in evidence. In the first situation a dense cloud of point is observed in a region of the plot, which according to the considerations just made, are most likely to be associated with wind sea states. Neverthless there also points with lower directional spread and steepness that fall under the swell domain. Apparently the wind sea misinterpretation introduced in section d finds a basis with this analysis. Viceversa in the case of the swell systems, a more consistent representations is given for MuSeas estimation (lower panel), where ECMWF does not recognize swell there might be a link with the swell underestimation observed in the scatter plot.

3) Characteristic frequency

A further assessment is obtained establishing the characteristic frequency from the wave age criterion (eq. 1), a generic estimation is thus given:

$$f_{ch} = \frac{g}{\alpha 2\pi U cos(\theta - \varphi)} \tag{6}$$

Integrating wave energy over the directions yields to 1D energy spectrum expressed as function of frequencies. A single spectrum was extracted from the misinterpreted wind sea cluster and plotted as follows in figure 8. If the characteristic frequency is superimposed then from the profile is possible to acquire information about the splitting mark between wind sea and swell. In the spectrum of 1 March 1990 12 UTC the position of the characteristic frequency suggests that most of the area is associated with swell frequencies, however a portion of higher frequencies is moving under the influences of wind sea. The example here proposed confirms how complicated can be the assignment process.

4. Conclusions

A spectral partitioning has been used to separate wave systems. The watershed algorithm has proven to be robust and it has been applied to a hindcast dataset for a location in the Norwegian Sea. The resulting statistics relative to the wave systems climate is examined with particular attention to the directional distributions. Uncertainties appear for the assignment to wind sea and swell components, as in real situations occur. As also noticed by Aarnes and Krogstad (2001) this process cannot be completely automatic but it relies on manual interaction. This lack of automatization can represent a serious problem when dealing, as in this case, with a large dataset. Emphasis was given to different possible options available for assignment, including different formulations for the governing wave age equation and a comparison with ECMWF results, which are obtained with a different technique. Additional criteria, based on directional spreading and wave steepnees have been proposed and demonstrated to be functional for the interpretation. As last contribution an attempt to include the characteristic frequency is also made.
Future work will deal with the joint descriptions of wind sea and swell systems. In this paper it has been stressed that the choice of different criteria will influence the final parameters distributions, therefore also the multivariate analysis will be affected.

Acknowledgments

This study was supported by the Marie Curie RTN SEAMOCS (MRTN-CT-2005-019374). Wave data were provided by ECMWF. D. Lucas and J. Bidlot are kindly acknowledge. L.L. thanks P. Osuna for fruitful discussion.

References

Aarnes, J. E. and H. E. Krogstad, 2001: Partitioning sequences for the dissection of directional ocean wave spectra: A review, Part of work package 4 (Wp4) of the EnviWave (EVG- 2001-00017) research program.

Bidlot, J. R., 2001: ECMWF wave-modelproducts, ECMWF Newsletter No. 91.

Bradbury A.P., T.E. Mason, T.Poate, 2007: Implications of the spectral shape of wave conditions for engineering design and coastal hazard assessment- Evidence from the English Channel. *In 10th International Workshop on Wave Hindcasting and Forecasting*, North Shore, Pahu, Hawaii.

Ewans K., E. Bitner-Gregersen, C. Guedes Soares, 2006: Estimation of wind-sea and swell components in a bimodal sea state. *Journal of Offshore Mechanics and Arctic Engineering*, **128**, 265 -270.

Gerling, T. W., 1992: Partitioning sequences and arrays of directional ocean wave spectra into component wave systems, *J. Atmos. OceanicTechnol.*, **9**, 444-458.

Goda, Y., 2000: Random seas and design on marine structures. *Advanced Series on Ocean Engineering*, **15**, World Scientific Pub. Co.

Hanson, J. L. and O. M. Phillips, 2001: Automated analysis of ocean surface directional wave spectra. *J. Atmos. OceanicTechnol.*, **18**, 277-293.

Hasselmann, S., C. Bruening, K. Hasselmann and P. Heimbach, 1996: An improved algorithm for retrievalofocean wave spectra from synthetic aperture radar image spectra. *J. Geoph. Res.*, **101(C7)**, 16615-16629.

Jonathan, P., K. Ewans , G. Forristal, 2008: Statistical estimation of extreme ocean environments: The requirement for modelling directionality and other covariate effects. *Ocean Engineering*, **35**,1211-1225.

Loffredo, L., 2009: MuSeas, a MATLAB toolbox for wave climate analysis. *Int. Rep. Hydraulics Laboratory*, Katholieke Universiteit Leuven (in prep.).

Portilla, J., F.J. Ocampo-Torres and J. Monbaliu, 2009: Spectral partitioning and identification of wind sea and swell. *J. Atmos. OceanicTechnol*, **26**, 107-122

Quentin, C., 2002: Etude de la surface ocèanique, de sa signature radar et de ses interactions avec le ux turbulent de quantitè de mouvement dans le cadre de l expèrience FETCH, Thèse de lUniversitè Paris 6. (in french)

Simmons, A., S. Uppala, D. Dee, S. Kobayashi, 2006: ERA-Interim: New ECMWF reanalysis products from 1989 onwards. ECMWF Newsletter No. 110.

Toffoli, A. and Lefèvre, J.M. and Bitner–Gregersen, E. and Monbaliu, J., 2005: Towards the identification of warning criteria: analysis of a ship accident database. *Applied Ocean Research*, **27**, 281-191.

Voorrips, A. C., V. K. Makin and S. Hasselmann, 1997: Assimilation of wave spectra from pitch- and-roll buoys in a North Sea wave model, *J. Geoph. Res.*, **102(C3)**,5829-5849.

WMO, 1998: Guide to wave analysis and forecasting. WMO-No 702